

SEM imaging of chiral nematic films cast from cellulose nanocrystal suspensions

Johanna Majoinen · Eero Kontturi · Olli Ikkala ·
Derek G. Gray

Received: 13 April 2012 / Accepted: 5 June 2012 / Published online: 26 June 2012
© Springer Science+Business Media B.V. 2012

Abstract The chiral nematic self-assembly of aqueous suspensions of cellulose nanocrystals is partially preserved on evaporation of water, but the ordering of the rod-like nanoparticles may become distorted by changes in volume, ionic strength and surface and convective forces during evaporation, thus affecting the morphology and optical properties of the dried film. Proposed applications for these solids with chiral nematic order require confirmation of their structure. A SEM examination of the fracture surface of a slowly-dried film showed a surprisingly regular fan-like pattern which is shown to be characteristic of cross-sections of the left-handed helicoidal arrangement of nanocrystals, where the helicoidal axis was almost perpendicular to the film surfaces. Superimposed on this pattern was what appeared to be a regular

porosity, which is postulated to result from pull-out of the nanocrystals oriented orthogonal to the fracture surface.

Keywords Cellulose nanocrystals · Electron microscope images · Chiral nematic films · Left-handed helicoidal structures · Film cross-sections · Fracture surface

Introduction

Cellulose nanocrystals (CNCs) can be produced by hydrolysis with strong acids from a number of different sources of cellulose including plants, bacteria and some sea animals (tunicates) (Habibi et al. 2010; Klemm et al. 2011). The highly crystalline rod-like CNCs in this study were produced from cellulose filter paper when sulfuric acid destroyed the amorphous parts of the cellulose fibrils. Charged sulfate half-ester groups are created on the CNC surface during the hydrolysis, and the resultant electrostatic repulsion between individual nanocrystals helps keep the CNCs well dispersed in water, hence producing a stable colloidal dispersion of rod like nanoparticles. Above a critical CNC concentration, this dispersion separates spontaneously into an isotropic phase and an anisotropic chiral nematic (cholesteric) liquid crystalline phase (Revol et al. 1992). Revol et al. (1992) also

J. Majoinen · O. Ikkala
Molecular Materials, Department of Applied Physics,
Aalto University, P. O. Box 15100, 00076 Aalto,
Espoo, Finland

E. Kontturi
Department of Forest Products Technology,
Aalto University, P. O. Box, 16300, 00076 Aalto,
Espoo, Finland

D. G. Gray (✉)
Department of Chemistry, McGill University,
Pulp and Paper Bldg., 3420 University Street,
Montreal, QC H3A 2A7, Canada
e-mail: derek.gray@mcgill.ca

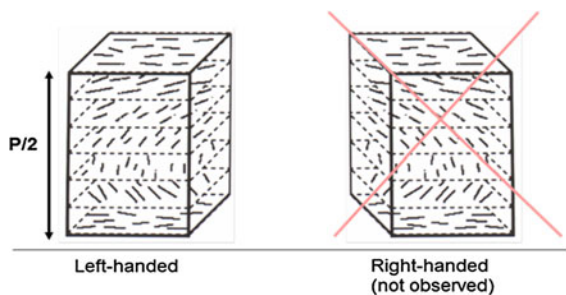


Fig. 1 Sketch of chiral nematic arrangement of cellulose nanocrystals

described how the colloidal liquid crystalline phase can be preserved in a solid film on slow evaporation of water, and they observed the mesophase structure in oblique sections of the solid film by transmission electron microscopy (TEM). Chiral nematic phases have been observed for concentrated solutions and melts of many cellulose derivatives (Gray 1995). Both left- and right-handed solutions, melts and films have been observed for cellulose *derivatives*, but to date only left-handed helicoids, first reported by Giasson (1995), have been observed for cellulose nanocrystal suspensions and films (Fig. 1). The assignment of handedness was based on TEM images of oblique microtomed sections of films cast from aqueous suspensions of cellulose nanocrystals, following the interpretation of the arcing observed in natural composites by Bouligand (2008). For a uniform planar texture, where the axis of the helicoid is at a 90° angle to the film surface, a cross-section through the film normal to the surfaces will show a quasi-layered structure, with the orientation of the nanocrystals progressing repeatedly from parallel to perpendicular to the cross-section. No arcing is observed. However, if the cross-section is made at an oblique angle to the helicoidal axis, arcing is observed (Fig. 2), with the shape of the arcs depending on whether the helicoidal arrangement is right-handed or left handed, and whether the oblique angle is greater or less than 90° (Fig. 3). The arcing observed for thin oblique sections of planar chiral nematic nanocrystal films by TEM indicates a left-handed helicoidal arrangement, but the technique requires very delicate sectioning and imaging to avoid electron beam damage to the unstained thin sections. Scanning electron microscopy allows

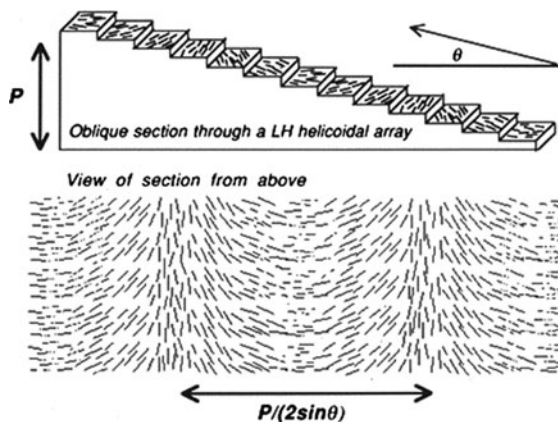


Fig. 2 Oblique section through the chiral nematic structure generates arc-like appearance

simple specimen preparation and ease of imaging of the dry film fracture surfaces at high resolution.

Experimental

Cellulose nanocrystals (CNCs) were prepared from ground cotton filter paper (Whatman 541) by sulfuric acid hydrolysis, according to the method of Edgar and Gray (2003). The average dimensions of the nanocrystals (~ 7.5 nm thick by ~ 150 nm long) were in accord with literature values (Elazzouzi-Hafraoui et al. 2008; Majoinen et al. 2011). The sulfate half-ester groups on the surface were in the acid form. The sulphate half ester content was estimated from an elemental sulphur analysis of the nanocrystals with a LECO SC-444 Sulfur and Carbon analyzer (LECO, St Joseph, MI). This gave an elemental S/C mass ratio of 0.015, from which an approximate degree of surface substitution of 0.1 was estimated from the dimensions of the nanocrystals. Cast films, ~ 70 μm thick, were prepared by slow evaporation over a few days of water from 1 to 2 wt% aqueous suspensions of cellulose nanocrystals under ambient conditions in a flat-bottomed Teflon[®] dish. The somewhat brittle films were fractured by bending, and the film cross-sections were coated with a thin Pt/Au layer. Scanning electron microscope (SEM) images at magnifications from $750\times$ to $120,000\times$ were acquired with a JEOL JSM-7500F scanning electron microscope operating at 2 kV and working distance 5.7 mm. The photomicrograph was imaged with a Leica Polarized Optical Microscope between crossed polars.

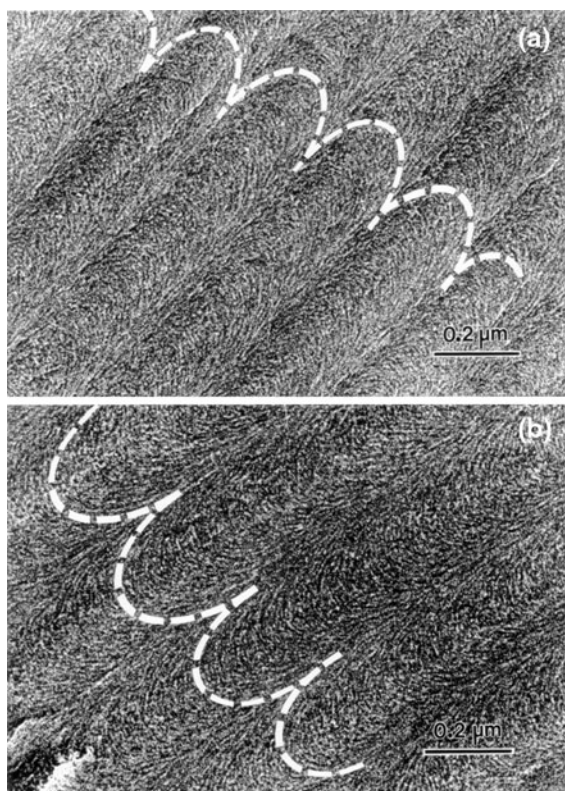


Fig. 3 Arcing observed in TEM images of thin oblique cross-sections through a planar chiral nematic film of wood cellulose nanocrystals cast from aqueous suspension on a Teflon[®] substrate. The sections were cut at angles such that the top left-hand corner of the image was tilted **a** towards and **b** away from the observer. Section thickness, 70 nm (Giasson 1995)

Results and discussion

When the cast CNC film is viewed in transmission between crossed polars in an optical microscope (Fig. 4a) the film shows the usual multidomain structure, where the direction of the chiral nematic axis changes with location in the film. In places, fingerprint lines characteristic of chiral nematic regions viewed orthogonal to the chiral nematic axis are in focus. The shortest distance between the lines is $P/2$, where P is the chiral nematic pitch. From the spacings in Fig. 4a, $P/2$ is in the range 1–3 μm . More diffuse and wider spaced lines are also apparent in Fig 4a. These correspond to positions where the chiral nematic axes are oriented at an angle to the surface. The observed colors are primarily due to interference generated by the birefringence of the film, and not by

chiral nematic reflection, as the P values are greater than the wavelength of visible light in the film.

Unmodified CNC films are brittle, and can be easily fractured. A SEM image of a fracture cross-section of the film is shown in Fig. 4b. The orientation of the chiral nematic axis is again seen to vary with position; on the left side of the image, the regularly spaced fingerprint lines indicate that the axis is almost perpendicular to the film surface, and the spacing corresponds to a $P/2$ value of $\sim 1 \mu\text{m}$, in good agreement with the value from optical microscopy. Again, areas with more diffuse lines are visible; these correspond to regions where the chiral nematic helicoid intersects the fracture surface at an oblique angle.

This interpretation is confirmed by the high resolution images shown in Fig. 4c and d. Figure 4c shows a higher magnification image of the layered structure, and the nature of the layers is apparent in Fig 4d, in which the orientation of the nanocrystals is clearly seen. The fan-like appearance corresponds to the cross-section of a left-handed helicoidal arrangement of nanocrystals, with the axis of the helicoid from top to bottom of the image. Note that the pattern results from a section through the spontaneous twist deformation of the drying suspension, and not from bend or play deformations (Bouligand 2008).

A striking feature of the SEM images in Fig. 4c and d is the apparent array of “holes” arranged in layers of the film cross-section. These appear at the position where the nanocrystals are oriented perpendicular to the fracture surface, and suggest that the higher strength of the film along the length direction of the nanocrystals results in pull-out of the nanocrystals oriented in this direction. If this is correct, then for every “hole” there should be an equivalent “hill” on the other fracture surface; in fact careful examination of Fig 4c shows that there do seem to be high spots just to the left and slightly below many of the holes; typical “hills” are marked by white arrows in Fig 4. This pattern is distinct from the extended array of parabolic focal conic disclinations that has been observed by polarized light microscopy in somewhat thinner cellulose nanocrystal films (Roman and Gray 2005). At the short length scales of the high resolution TEM images reported here, there is no clear evidence of disclinations (i.e., regions where the orientation of the nanocrystals is indeterminate).

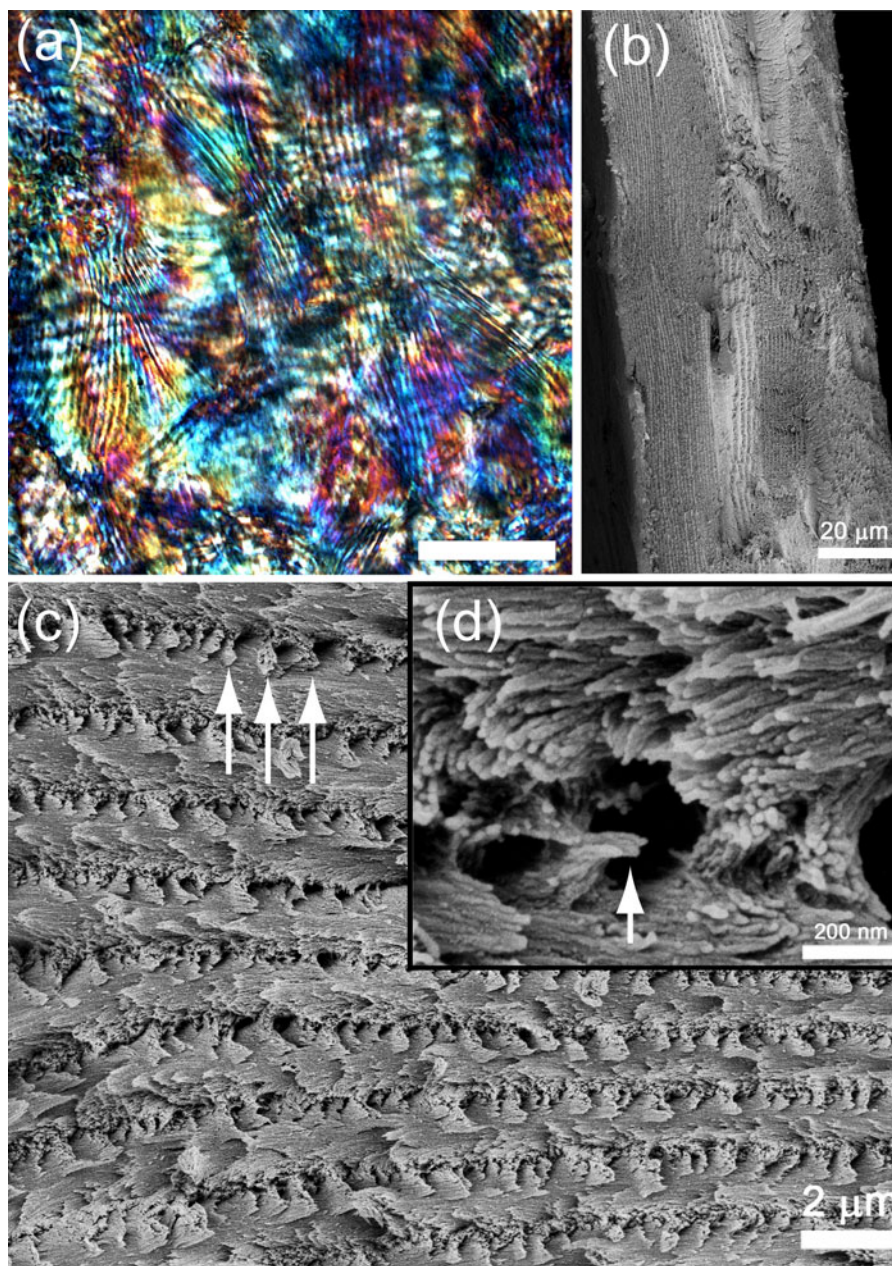


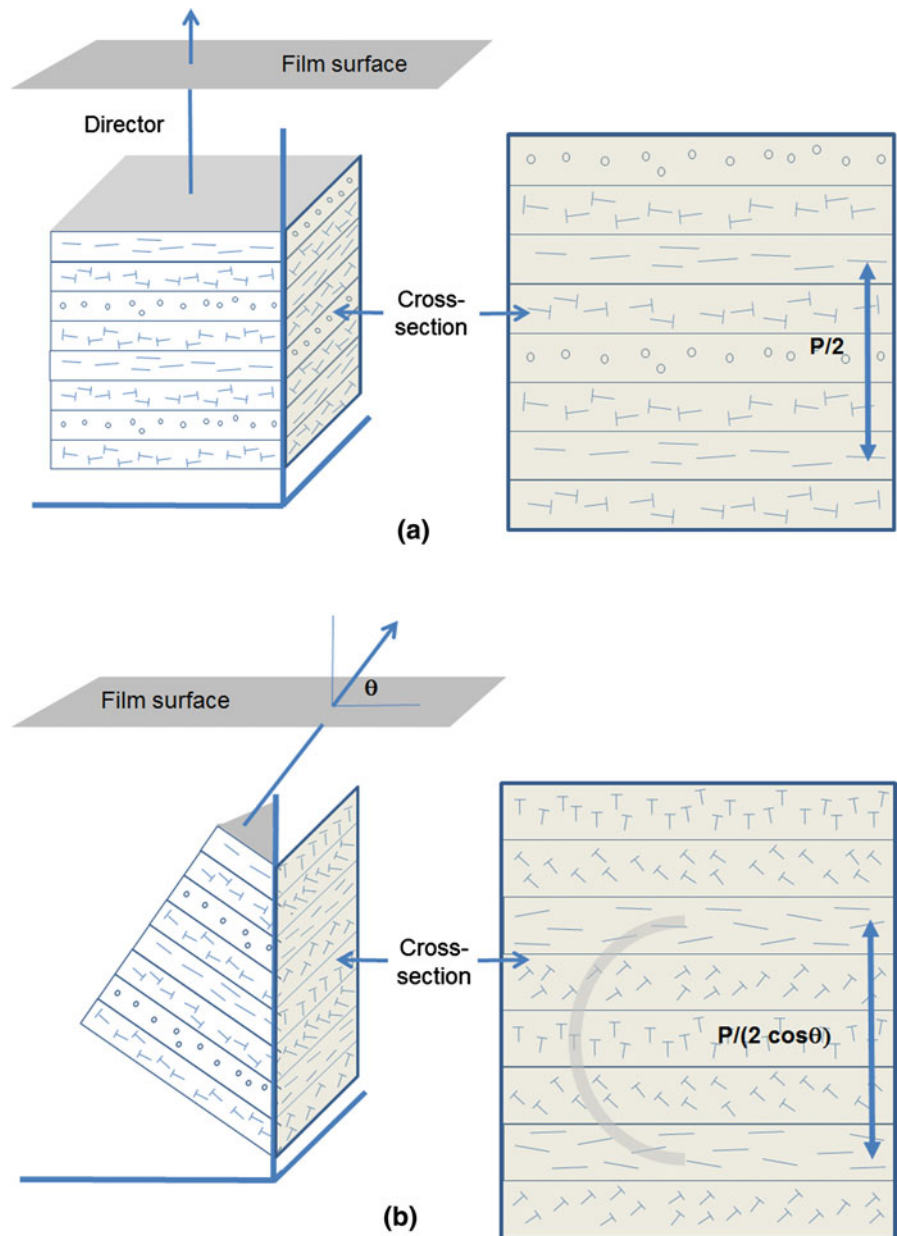
Fig. 4 **a** Optical microscope image (crossed polars) of the bulk CNC film (*scale bar* 40 μm), **b**, **c** and **d** SEM images of a fracture surface across the film. In **c** and **d** the film is oriented

horizontally. The *white arrows* in **c** and **d** indicate examples of nanocrystal bundles pulled above fracture surface

Interpretation of the orientation of the nanocrystals in the fracture surface is worth considering further. The fan-like arcing pattern visible in Fig. 4d resembles that observed in oblique sections (Fig. 3), but in the SEM images, it is the chiral nematic axis that is at an angle to the fracture surface. This is illustrated in

Fig. 5, in which the orientation of the nanocrystals is represented by a nail convention for representing a three-dimensional orientation in two dimensions (Bouligand 1999). Here, for a left-handed structure, the nail head is oriented away from the observer in Fig. 5. When a section is cut parallel to the chiral

Fig. 5 Cross-sections of a left-handed chiral nematic structure, planar texture **a** director normal to film surface **b** director tilted relative to film surface



nematic axis, no arcing is apparent (Fig. 5a). On tilting the helicoidal structure such that the chiral nematic axis is at an angle to the cut, arcing becomes visible. When the chiral nematic axis is tilted towards the section surface, the arcing takes a C shape (Fig. 5b); if the top of the helicoid is tilted away from the surface, D-shaped arcing results.

The interpretation of the fan-like texture observed by SEM of a fracture surface is thus in line with a

normal chiral nematic helicoidal arrangement. As shown in Fig. 6, line DE lies along a projection of the chiral nematic axis onto the fracture surface. From the out of plane orientation of the nanocrystals, indicated by the nail convention, the nanocrystals form a left-handed helicoid. In analogy with the arcing observed for the thin TEM sections (Fig. 3), the D-shaped segments of arcs AB and AC indicate that the chiral nematic axis projects onto the line DE such that the

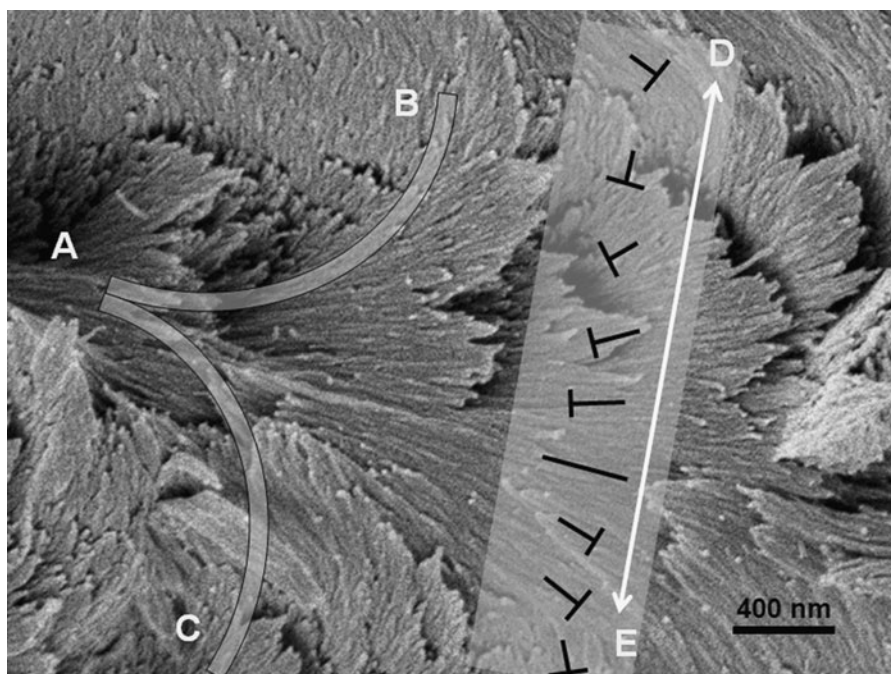


Fig. 6 Interpretation of a SEM image of the fracture surface of a cellulose nanocrystal film. DE indicates a projection of the chiral nematic axis onto the plane of the fracture surface. The out of plane orientation of the cellulose nanocrystals is indicated

by the nail convention, where the tip of the nail is projecting above the plane. The apparent arcing AB, AC results from the out of plane orientation of the chiral nematic axis

axis is further from the surface at E than at D. Thus the pitch, handedness and orientation of the helicoidal axis can be determined from the TEM image.

The chiral nematic structure of cellulose nanocrystal suspensions above the critical concentration is an equilibrium state, with a pitch that is essentially dependent on nanocrystal concentration, geometry and electrostatic charge (Dong et al. 1996). However, it is important to recognize that, as more and more water is removed, a point is reached where the nanocrystals no longer can achieve their equilibrium conformation, because further increase in relative twist between nanocrystals as their number density increases is inhibited by instability. Thus equilibrium theories proposed to explain the effects of concentration, ionic strength and temperature on the helicoidal pitch and reflection colours displayed by lyotropic and thermotropic liquid crystals no longer apply to the films. The point at which the orientation becomes jammed will depend on many factors, including nanocrystal geometry, initial concentration, rate of evaporation, surface charge and ionic strength.

Nevertheless, under the conditions used to make the NCC films here, a frozen-in chiral nematic arrangement is clearly preferred. The significance of the ordering and drying process extends beyond cellulosic materials. By using cellulose nanocrystals as a template for the chiral self assembly of a silica sol-gel precursor, and then calcining at elevated temperatures, a porous inorganic silica with a chiral nematic distribution of voids gives a glass with reflection bands (Shopsowitz et al. 2010), similar to those observed for cellulose nanocrystal films (Revol et al. 1992). Furthermore, silica can be selectively removed from the sol-gel precursor to give a porous carbon, again with a chiral nematic ordering of anisotropic voids (Shopsowitz et al. 2012).

Conclusion

The SEM images of the film fracture surface give a clear indication of the pitch, handedness and direction of the chiral nematic director and other details of

cellulose nanocrystal film structure. Combined with the early TEM images of thin oblique sections, the images show that slow evaporation of the chiral nematic suspensions of cellulose crystallites results in a surprisingly well-ordered local chiral nematic structure in the dry films. The results also demonstrate that high-resolution SEM of cellulose nanocrystal films can give information on the detailed structure and failure mechanisms of this model chiral nematic system. The apparent porosity in the fracture surfaces reported here may result from pull-out of nanocrystals oriented orthogonal to the fracture surface. This information provides a basis for the exploitation of the unusual optical and templating properties of these materials.

Acknowledgments We thank Dr. Mari Granström for insightful discussions. The work of J. Majoinen, E. Kontturi and O. Ikkala was supported by the Finnish Funding Agency for Technology and Innovation (TEKES) and Academy of Finland, as part of the Finnish Center of Nanocellulose, a joint project of Aalto University, UPM, and VTT. DGG thanks NSERC Canada and the Centre for Self-assembled Chemical Structures for support

References

- Bouligand Y (1999) Defects and textures, chap 7. In: Demus D, Goodby J, Gray GW, Speiss H-W, Vill V (eds) *Physical properties of liquid crystals*. Wiley-VCH, Weinheim, pp 305–350
- Bouligand Y (2008) *Liquid crystals and biological morphogenesis: ancient and new questions*. C. R. Chimie 11: 281–296 and references cited therein
- Dong XM, Kimura T, Revol J-F, Gray DG (1996) Effects of ionic strength on the phase separation of suspensions of cellulose crystallites. *Langmuir* 12:2076–2082
- Edgar CD, Gray DG (2003) Smooth model cellulose I surfaces from nanocrystal suspensions. *Cellulose* 10(4):299–306
- Elazzouzi-Hafraoui S, Nishiyama Y, Putaux J-L, Heux L, Dubreuil F, Rochas C (2008) Shape and size distribution of crystalline nanoparticles prepared by acid hydrolysis of native cellulose. *Biomacromolecules* 9:57–65
- Giasson J (1995) *Études microscopiques d'hélicoïdes de systèmes cellulosiques in vitro*. Dissertation, McGill University, Ch. 5, p 167
- Gray DG (1995) Chiral nematic ordering of polysaccharides. *Carbohydr Polym* 25(4):277–284
- Habibi Y, Lucia LA, Rojas OJ (2010) Cellulose nanocrystals: chemistry, self-assembly, and applications. *Chem Rev* 110:3479–3500
- Klemm D, Kramer FS, Moritz S, Lindström T, Ankerfors M, Gray D, Dorris A (2011) Nanocelluloses: a new family of nature-based materials. *Angew Chem Int Ed* 50:5438–5466
- Majoinen J, Walther A, McKee JR, Kontturi E, Aseyev V, Malho JM, Ruokolainen J, Ikkala O (2011) Polyelectrolyte brushes grafted from cellulose nanocrystals using Cu-mediated surface-initiated controlled radical polymerization. *Biomacromolecules* 12(8):2997–3006
- Revol J-F, Bradford H, Giasson J, Marchessault RH, Gray DG (1992) Helicoidal self-ordering of cellulose microfibrils in aqueous suspension. *Int J Biol Macromol* 14:170–172
- Roman M, Gray DG (2005) Parabolic focal conics in self-assembled solid films of cellulose nanocrystals. *Langmuir* 21(12):5555–5561
- Shopsowitz KE, Qi H, Hamad WY, MacLachlan MJ (2010) Free-standing mesoporous silica films with tunable chiral nematic structures. *Nature* 468:422–425
- Shopsowitz KE, Hamad WY, MacLachlan MJ (2011) Chiral nematic mesoporous carbon derived from nanocrystalline cellulose. *Angew Chem Int Ed* 50:10991–10995